NEW MULTIBEAM BEAMFORMING NETWORKS FOR PHASED ARRAY ANTENNAS USING ADVANCED MMCM TECHNOLOGY

F. COROMINA[1] - J VENTURA-TRAVESET[1] - J.L. CORRAL[1] - Y. BONNAIRE[2] - A. DRAVET[2]

[1] ESA-ESTEC
PO Box 299, 2200 AG NOORDWIJK
The Netherlands

[2] DASSAULT ELECTRONIQUE
55 Quai Marcel Dassault
92214 - SAINT CLOUD France

ABSTRACT

A new concept for the implementation of complex RF beamforming networks (BFN) based on Microwave MultiChip Module (MMCM) technology, including MMICs and 3D multilayer structure is presented. Its validity is fully demonstrated by the fabrication and characterization of a S-Band 9x9 beamformer using low cost, low mass space qualifiable processes and exhibiting remarkable RF performances.

INTRODUCTION

Future communication satellites for mobile service applications will make use of active antennas with a very high number of radiating elements and beams. Classical RF BFNs are not convenient for these applications, due to their high associated mass and dimensions. A new concept is proposed for their implementation. It allows a very dense grid of fixed beams for array antennas with a very high number of radiating elements distributed along a hexagonal grid. This BFN allows very low mass and dimensions, very high manufacturing yield with very low manufacturing cost.

BFN ARCHITECTURAL CONCEPT

The multibeam beamformer architecture actually performs the Discrete Fourier Transform (DFT) of a bidimensional sequence hexagonally sampled (which corresponds to the signal inputs at the antenna elements, which are hexagonally distributed on the antenna aperture), such that the resulting coefficients of the DFT are also hexagonally sampled in the transform domain (corresponding to a hexagonally distributed beam grid). Considering hardware efficiency criteria (modularity, row-column decomposition, minimum number of fixed phase shifters, ...), a general mathematical procedure based on the theory of lattices and multidimensional signal processing techniques, ([1] [2] and [3]), has been applied for the generation of the beamformer architecture. This procedure is applicable to a large variety of hexagonal grid beamformers. As an implementation example, a 81 beam/81 element beamformer architecture is shown Fig. 1. The structure is based on a 9x9 BFN unit (Fig. 2) which is made of basic 3x3 cells (implemented in MMIC form) interconnected by a complex multilayer structure including delay lines as narrow band phase shifters. The 3x3 cells have 3 inputs and 3 outputs. The signal present at any input is equally split to the three outputs, and the relative phase of the 3 output signals depends on the input port as shown in the table Fig. 3.

DEMONSTRATOR

One 9x9 BFN unit as shown Fig. 2 has been designed, manufactured and tested. The frequency of operation is 2.3 GHz. Each 3x3 cell is implemented in MMIC form.

The layout of this MMIC is given Fig. 4. As it can be seen from the figure, the MMIC is a fully passive network, made of inductors and capacitors. Each of the capacitors includes a cold

0-7803-3246-6/96/$5.00 © IEEE

FET working as a variable capacitor. The role of these variable capacitors is to compensate for the systematic wafer dependant capacitance error. Assuming that all the MMICs used in the 81x81 BFN come from the same wafer, a single control voltage is needed for the compensation of all the capacitors in the BFN. The capability of electronically tuning the wafer dependant capacitor error leads to a successful single iteration design. It is assumed that the inductors are very well controlled and repeatible elements in any good MMIC foundry process. As well, due to the simplicity of the MMIC circuit, a very high manufacturing yield is obtained. This MMIC has been designed and manufactured using the D02AH P-HEMT process from PHILIPS-LIMEIL.

Concerning the interconnection multilayer structure, the need for minimum dimensions, (determined by the necessary input/output connectors), together with the requirement of good RF isolation (better than 40 dB) between the different RF lines, led to a structure involving 4 stripline layers interconnected with metallized via holes (Fig. 5)

Standard 6002 Duroïd technology from Rogers Corp. has been selected for the 9x9 BFN demonstrator manufacturing with respect to high electrical performance, minimum layer thickness and technology maturity.

Main physical properties of 6002 Duroïd process are as follows :

- Layer thickness : 0.127 mm
- Dielectric constant (10 GHz) : 2.9
- Dissipation factor (10 GHz) : 0.0013
- Thermal exp. ppm/°C : 16 (X/Y) - 24 (Z)

DASSAULT ELECTRONIQUE has been using this technology for more than 10 years in the field of commercial, military and space applications. In particular, 6002 Duroïd process has been proven to meet thermal shocks requirements of ESA specifications (500 thermal shocks from -55°C to +125°C). Figure 6 shows the process flow chart which has been used for multilayer board fabrication. MMICs are glued into the cavities of the multilayer board with a flexible conductive epoxy.

Regarding RF line routing, the main objective was to tightly control the insertion phase of the interconnection striplines. Electromagnetic simulations were carried out using the SONNET CAD tool. For such a circuit topology, the main effects which have to be simulated are the parasitics due to stripline bends and coupling between lines. It was found that a typical stripline lenght correction of -0.5 mm had to be applied for each stripline bend and for each coupled line section.

Figure 7 represents the photograph of the 9x9 S-band MMCM Beamformer including the view of the different RF layers. The 9x9 Beamformer dimensions are 110mm x 13mm x 2mm (4.4"L x 0.5"W x 0.08"H). The total microwave line length embedded in this structure is 1.5 m (5'), corresponding to about 2.5 m (8.2') in air. It weights less than 30 g (1.1 oz.), leading to a whole 81/81 structure of less than 1 kg (2.2lb.), compared to 25 kg (55 lb.) for a classical beamformer.

MEASUREMENTS RESULTS

A first set of measurements was performed using the multilayer structure and substituting the MMICs by 3 thru connections using 50 ohm lines. With the 50 ohm thru connections, every "Ei" input is connected to the "Si" output and isolated from all the other outputs. It can be seen that RF transmission losses of around 1.7 dB have been obtained, with 0.6 dB peak to peak variations (amplitude tracking), together with worst case RF isolation of 40 dB. Concerning phase, a worst case phase error of 10 degrees in one input to output path was measured. These results show very good performance in terms of losses and isolation. Amplitude and phase errors are very good for a first design iteration, given the high complexity and compactness of the structure. In a second design iteration, an excellent phase and amplitude tracking can be achieved.

As second set of measurements was performed with all the 9 MMICs installed. Concerning phase errors, Fig. 8 shows the phase errors with respect to the ideal values after capacitance tuning using the single control voltage and after some output phase compensation using delta line

lengths at the 9 BFN outputs : the need for this line length compensation arose due to the phase errors on the stripline lines on the multilayer structure and to some phase errors on the measured MMIC performance. In a second iteration of the BFN, such a correction will not be necessary. A measured rms phase error of 5 degrees rms (calculated through all beam inputs and radiating elements outputs) has been obtained. Concerning insertion losses, a mean value of 21.5 dB (including 9.5 dB splitting loss) and 0.7 dB rms amplitude variation have been obtained.

With the phase and amplitude test results of the 9x9 BFN, simulations have been made of the radiation pattern characteristics of the 81 beams generated by the 81x81 BFN (Fig. 1) driving a 37 element hexagonal grid phased array antenna (no antenna amplitude taper is implemented after the BFN). The mean value of the 81 worst sidelobe levels of each beam is 15 dB, with a sigma value of 0.7 dB. The ideal error free first sidelobe level of this antenna with uniform illlumination is of 15.8 dB.

CONCLUSION

A novel approach for the implementation of RF beamforming networks with a very high number of beamforming nodes has been demonstrated. It exhibits extremely low mass and dimensions, together with high success after the first design. The S-Band 9x9 Beamformer with MMCM technology was manufactured within 9 months total design, manufacturing and test cycle. The built demonstrator, using low cost, low mass, space qualifiable technologies and giving remarkable RF performances, has demonstrated the validity of this new concept of RF beamformer that could be useful in several applications as for example BFNs for LEO (Low Earth Orbit) satellites for mobile communications.

REFERENCES

[1] "The Processing of Hexagonally Sampled Two-Dimensional Signals", by Russell M. Mersereau, in Proceedings of the IEEE, Vol 67, N° 6, June 1979.

[2] "The Processing of Periodically Sampled Multidimensional Signals", by Russell M. Mersereau and Theresa C. Speake, in IEEE Transactions on Acoustics, Speech and Signal Processing, Vol. ASSP-31, N° 1, February 1983.

[3] "Fast Algorithms for the Multidimensional Discrete Fourier Transform", by Abderrezak Guessoum and Russel M. Mersereau in IEEE Transactions on Acoustics, Speech and Signal Processing, Vol. ASSP-34, N° 4, August, 1986.

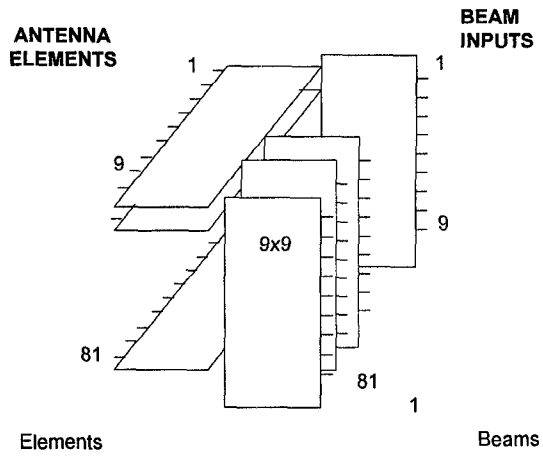

Figure 1 : 81 beam/81 element beamformer architecture

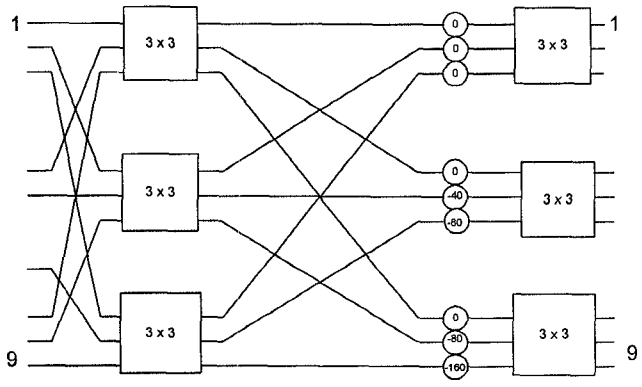

Figure 2 : Block Diagram of a 9x9 BFN unit

Out / In	4	5	6
1	120	0	0
2	0	120	0
3	0	0	120

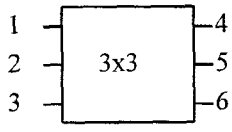

Figure 3 : 3x3 MMIC cells
Relative phase for output signals corresponding to each input signal port

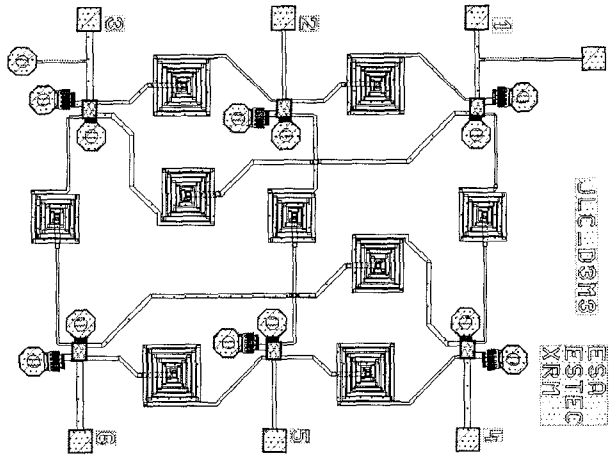

Figure 4 : Layout of the 3x3 coupler cell with MESFETs for capacitance error tuning

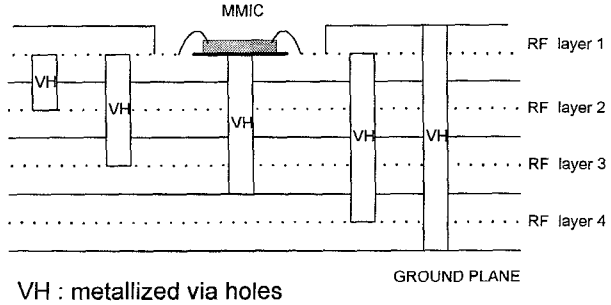

Figure 5 : Multilayer structure cross section

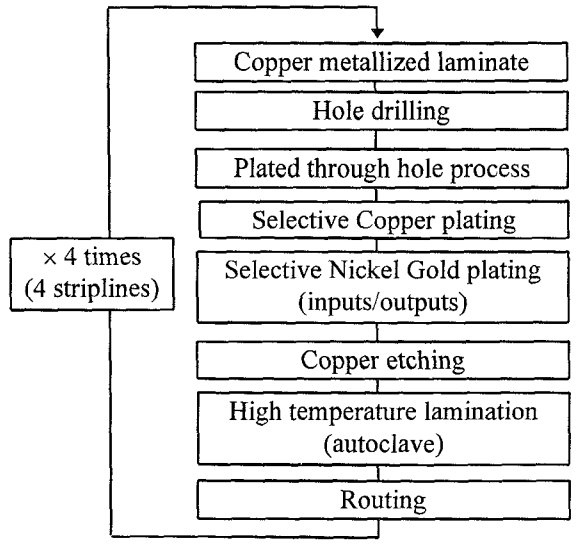

Figure 6 : Multilayer process flow chart

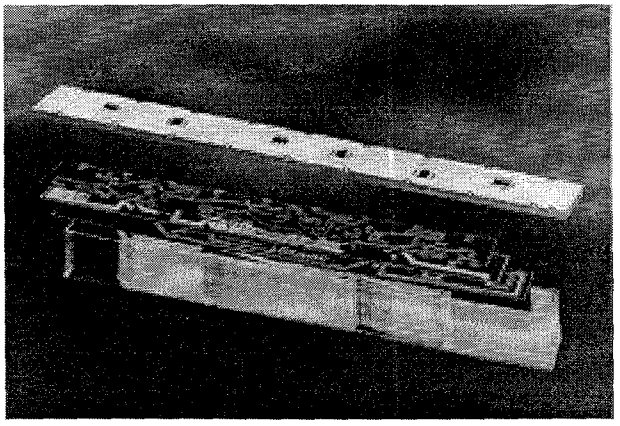

Figure 7 : 9x9 S-band MMCM Beamformer

	S1	S2	S3	S4	S5	S6	S7	S8	S9
E1	-5.1	1.4	-2.6	-3.4	7.1	-1.0	-3.0	9.2	-2.6
E2	1.7	-0.9	-1.9	1.3	-0.1	0.8	2.8	-2.0	-1.5
E3	-0.1	6.3	-7.7	0.5	5.1	-4.0	0.0	8.2	-8.3
E4	-0.6	2.9	1.9	5.1	-4.3	-10.5	4.5	-0.2	1.2
E5	6.1	-2.5	-1.5	1.8	-5.7	-1.8	7.2	-3.6	-0.1
E6	8.5	-1.0	-5.0	-1.8	1.8	-7.3	6.7	3.9	-5.6
E7	-11.0	4.4	8.4	-4.3	1.2	11.1	-6.9	-4.7	1.8
E8	-0.1	-8.7	6.3	0.5	-5.9	8.0	-3.0	-5.8	8.7
E9	0.7	-1.9	2.1	0.3	0.9	4.8	-8.2	-5.0	6.4

	E1	E2	E3	E4	E5	E6	E7	E8	E9	Total
rms	4.7	1.6	5.6	4.6	4.1	5.3	6.9	6.1	4.3	5.0

Figure 8 : Normalized measured phase value errors after output line insertion